The Physics of Low-Dimensional Structures

From Quantum Wells to DNA and Artificial Atoms

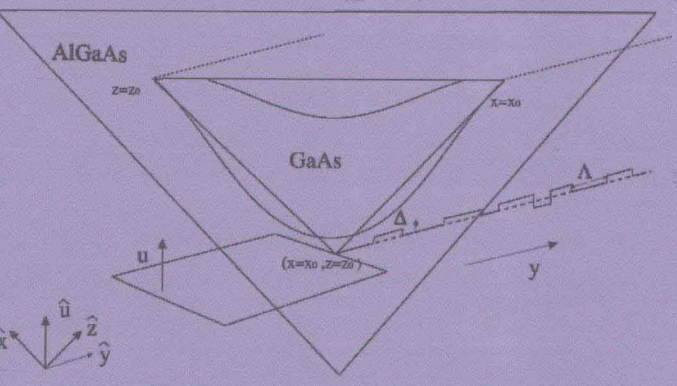

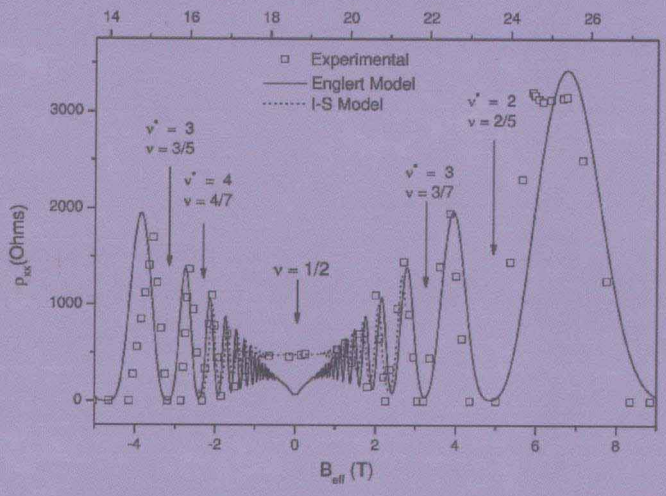

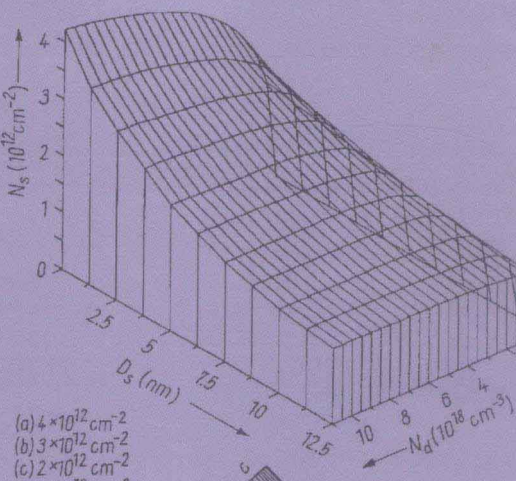

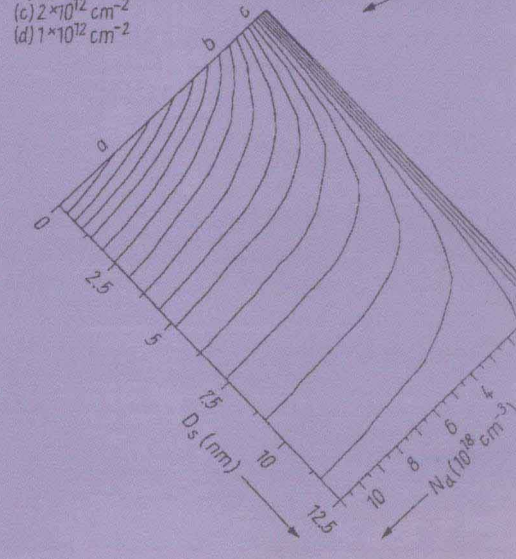

Georgios P. Triberis

NOVA

THE PHYSICS OF LOW-DIMENSIONAL STRUCTURES: FROM QUANTUM WELLS TO DNA AND ARTIFICIAL ATOMS

GEORGIOS P. TRIBERIS

Nova Science Publishers, Inc.
New York

Library of Congress Cataloging-in-Publication Data
The physics of low-dimensional structures : from quantum wells to DNA and artificial atoms / Georgios P. Triberis, editor.
p. ; cm.
Includes index.
ISBN 13 978-1-60021-477-6
ISBN 10 1-60021-477-0
1. Doped semiconductors. 2. Quantum wells. 3. Nanowires. 4. Quantum dots. I. Triberis, Georgios P. [DNLM: 1. Nanostructures. 2. Quantum Theory. 3. DNA–chemistry. QC 611.6.S9 P578 2006]
QC611.8.D66P59 2006
537.6'22–dc22 2006032326

Published by Nova Science Publishers, Inc. ✣ New York

Preface

This book covers the field of low dimensional structures, starting from the selectively doped double heterostructures $n-A_1GaAs/GaAs/n-A_1GaAs$, and (strained) $p-Si/SiGe/p-Si$ (quantum wells).

The behavior of the sheet electron density, the subband populations and energies as a function of the well width, the spacer thickness and the doping concentration is analyzed. The temperature dependence of the bulk electron concentration versus the quasi-2DEG are discussed.

In the framework of Boltzmann's transport theory a detailed study of the mobility is presented at low and high temperatures taking into account all the relevant scattering mechanisms.

The pseudomorphic Si/SiGe undoped quantum wells are a perfect example for the study of the non-parabolicity of the hole-bands. For the first time in a book an exact solution of the multiband effective mass equation that describes the heavy, light and split-off hole valence bands is introduced, and interband transitions and selection rules are obtained.

Reducing dimensionality new aspects concerning optical and transport properties of quantum wires (QWRS) is discussed. Specifically, the photoluminescence and the microphotoluminescence spectra of V-shaped QWRS is theoretically interpreted leading to a realistic cartography of the interface roughness of these systems. A computational approach for the solution of the eigenvalue problem in low-dimensional systems of complex but realistic geometry is also presented for the first time in a book, and transport theoretical considerations will lead to a systematic study of the mobility.

As DNA could be considered as a one-dimensional "molecular wire" the study of carrier transport along DNA is discussed in terms of hopping transport.

A computational scheme is presented which allows the study of near-field magnetoabsorpsion spectra of Quantum Dots (QD) of any given geometry, under magnetic field of any orientation. The effect of the spatial confinement imposed by the QD dimensions and the magnetic confinement governed by the magnetic field are explored. The influence of the Coulomb interactions between electrons and holes is also discussed. The applicability of the method in actual experiments, i.e. the illumination of a nanostructure with a near-field probe in conjunction with the simultaneous application of an external magnetic field, may become a challenge to experimentalists.

Finally, magnetothermoelectic transport in the fractional quantum Hall effect (FQHE) regime is discussed. The theoretical framework for the calculation of the resistivity, the thermopower and the thermal conductivity for two-dimensional electron and hole gases, at low temperatures and strong perpendicular magnetic fields is outlined. The composite

fermion picture enables the use of the integer quantum Hall effect and Shubnikov - de Haas conductivity models for a quantitative comparison with experiment. A study on the validity of fundamental physical laws such as the Wiedemann-Franz law in two-dimensional structures is also presented.

Introduction

From the time (1910) when Michael Faraday observed that the resistance of AgS was decreasing increasing temperature till the time we started ascribe certain and well defined physical properties to the semiconductors they were under doubt even aphorism.

"One should not work on semiconductors that is a filthy mess; who knows whether they really exist" (W. Pauli, 1931). The world of the semiconductors was not always so bright as it is in the beginning of the 21st century.

W. Smith [1] was the first who observed the photoconductivity , while F. Braun [2], using materials such as PbS observed the rectification. In 1879 the Hall effect was revealed [3]. The first systematic use of the Hall effect for semiconductor studies was performed by K. Bacdeger [4] and detailed studies of a variety of semiconducting materials were published by J. Königsberger [5]. The study of the chemistry of a number of semiconductor compounds led C. Wagner [6] to classify them as "defect" and "excess" semiconductors.

The development of the Quantum Theory and the Statistical Mechanics opened new windows for the understanding of the physics of semiconductors. A. H. Wilson and Walter Schottky were among the pioneers of that time. In the time period 1939-1945 organized semiconductor technology starts to grow. The real progress comes next with epicenters the Perdue University under Karl Lark-Horovitz and the Bell Telephone Labs under W. Shockley. In fifties it was possible to produce reliable semiconductor monocrystals, and the integrated circuits idea started to grow. The revolutionary bipolar transistor [7, 8] and the field effect transistor later push forward the semiconductor research.

It seems that the first efforts for the creation of p-n contacts consisting of different semiconductors come from the early fifties [9, 10]. The first attempts to built Ge/Si and Ge/GaAs in the beginning of sixties were unsuccessful [11, 12], due to the great number of defects in the interfaces, and this weakened the scientific interest in this direction. The research interest warmed up in 1970 after the succesful fabrication of a semiconductor contact laser, at room temperature based on a GaAs/AlGaAs double heterojunction [13]. The small difference of the lattice constants of these two materials resulted to the fabrication of good quality heterointerfaces.

The technological demands have driven to a systematic study of the semiconductor heterostructures. New alloy semiconductors appear and the idea of the development of artificial semiconductor heterostructures is born seeking for band structure control (band engineering) and of the concomitant properties. The progress in band gap engineering was based on the formation of alloys of two or more semiconductors, in order to create semiconductors with new band structure and specifically with a predetermined desired value

of the band gap.

Another new characteristic is the formation of semiconductrors with an appropriate lattice constant to grow over a specific substrate. The formation of heterointerfaces, less rough as possible, is also an essential element of these artificial structures. The two different semiconductors come in contact consisting a new unique physical system.

The different technics of heteroepitaxial crystal growth such as Molecular Beam Epitaxy, Metal-Organic Chemical Vapor Deposition (MOCVD), Ultrahigh-Vacuum Chemical Vapor Deposition (UHVCVD), Rapid Thermal Chemical Vapor Deposition (RTCVD)or Low-Pressure Chemical Vapor Deposition (LPCVD), contribute decisively to the progress of the technology of semiconductor heterostructures.

The conduction (or valence) band profile of these two semiconductors in contact presents band discontinuities at the interface which characterize the heterostructure. According to the relative position of the band extrema of the constituent materials the heterostrucrures are classified in different types (type I, II or III). The formation of heterointerfaces between semiconductors with different lattice constants results to the appearance of (built-in) strain which can be used as another controlling parameter for the band engineering. The periodic growth of consecutive layers of different semiconductors results to the formation of supperlattices where now the role of the lattice constant is played by the layer thickness while the atomic periodic potentials are substituted by the potential of the energy bands of the successive layers.

The formation of heterointerfaces results to the creation of confining potential of the carriers in one, two or three dimensions, creating the well known Quantum Wells (QWs), Quantum Wires (QWRs), or Quantum Dots (QDs), respectively.

A wide variety of semiconductor compounds have been used to achieve heterostructures with the desired characteristics. Among the most successful and widely studied are the $AlGaAs/GaAs$ and the $Si/SiGe$ heterostructures.

GaAs is one of the most important semiconductors with technological applications following the dominant Si technology. GaAs properties are unique and it becomes, along with its compounds, ideal for electronic and optoelectronic applications. Among other characteristics, the effective electron mass in GaAs at the Γ - point is very small (0.067 of the free electron mass), suitable for high speed devices. The difference in the lattice constants of GaAs and AlGaAs (0.14%) results to heterointerfaces AlGaAs/GaAs free of strain and of very good quality.

The basic reason for the delay of using Si and its compounds in heterostructures was the big difference ($\approx 4\%$) between the lattice constants of Si and Ge. Finally in 1984 Si/SiGe heterojunctions of good quality fabricated and for the first time the quasi-two dimensional hole gas was observed.

During the following years an enormous number of technological applications have been brought to light and new physical phenomena surprised and impressed us.

At the same time, looking for alternative semiconducting materials, the researchers have turn their attention to the study of the physical properties of bio-materials such as DNA, organic membranes etc.

The present book intents to guide you in a journey across certain interesting parts of the physical world of these low dimensional structures. It aims to reveal to you the beauty of physics behind of the bright surfaces of the mobile telephones and the other electronic

products without which some of us think that they can not survive. The book travels in time covering in a systematic way earlier research topics referred to QWs till very recent developments concerning V-shaped WQRs, charge transport along the DNA molecule, near field spectroscopy of QDs and fractional quantum Hall effect.

Specifically, **Chapter 1** is devoted to Quantum Wells.

Section 1.1. is focused on $n - Al_xGa_{1-x}As/GaAs/n - Al_xGa_{1-x}As$ Selectively Doped Double Heterostructures (SD-DH). In Subsection 1.1.1. a systematic analysis of their electron states is presented using an algorithm based on the simultaneous solution of the Schrödinger and Poisson equations. The dependence of the sheet electron concentration, and the subband populations on the well width, spacer thickness and doping concentration, at zero temperature, is discussed along with the transition from a "perfect" square well to a system of "two separated heterojunctions". In Subsection 1.1.2. a quantitative analysis attempts the interpretation of the temperature dependence of the Quasi-two Dimensional Electron Gas (Q2DEG) versus bulk sheet electron concentration and allows the determination of the Q2DEG and the bulk mobilities at any temperature. A full treatment of the low and high temperature electron mobility is also given in Subsections 1.1.3. and 1.1.4., respectively, taking into account all the relevant scattering mechanisms.

In going from $n - Al_xGa_{1-x}As/GaAs/n - Al_xGa_{1-x}As$ SD-DH to strained $p - Si/Si_xGe_{1-x}/p - Si$ there are considerable differences due to appearance of strain in the Si/SiGe interface.

Section 1.2. investigates the behavior of the strained $p - Si/Si_xGe_{1-x}/p - Si$ Selectively Doped Double Heterostructures. In Subsection 1.2.1. the effect of the material and the structural parameters on the hole states in these structures is presented. In Subsection 1.2.2. the low temperature hole mobility is discussed using a multisubband transport model. In Subsection 1.2.3. we study the hole subband non-parabolicities in undoped pseudomorphic $Si/Si_xGe_{1-x}/Si$ quantum wells, strained in the growth direction. We present the exact solution of the multiband effective mass equation that describes the heavy, light and split-off hole valence bands. The in-plane dispersion relations $E(k||)$ are produced. We also discuss the importance of the inclusion of the split-off hole valence band in the Hamiltonian. We comment on the resultant non-parabolicities and anisotropy of the hole subbands. In Subsection 1.2.4. we investigate the selection rules governing the optical transitions in p-type Si/SiGe quantum wells using a multiband effective-mass approach.

Lowering dimensions in **Chapter 2** we turn our attention to $AlGaAs/GaAs$ Quantum Wires (QWRs).

In Section 2.1. we present an approach for a study of the electron and heavy hole ground state of QWRs. In Subsection 2.1.1. the finite difference method to calculate the ground state of QWRs of different cross sections is presented. The reliability of the method is tested studying the influence of the wire's environment, experimental characteristics and other parameters involved. In Subsection 2.1.2. is applied to V-shaped QWRs, while in Subsection 2.1.3. rectangular QWRs are studied.

In Section 2.2. we present the theoretical model for the cartography of the interface roughness of V-Shaped QWRs which is reflected on the photoluminescence and micro-photoluminescence spectra of these structures. In Subsection 2.2.1. the theoretical (PL-analysis) framework is given for the interpretation of the PL-spectrum Subsection (2.2.3.). In Subsection 2.2.2. the corresponding theory (micro-PL analysis) is developed for the in-

terpretation of the micro-PL spectrum (Subsection 2.2.4.).

In Section 2.3. the low temperature mobility in V-shaped QWRs is investigated. The energy eigenstates and eigenvalues of the system are calculated using the finite difference method and the cartography of the interface allows for realistic values of the rms value of the roughness fluctuations in depth and the autocorrelation length. In Subsection 2.3.1. for one subband occupation the screened and the unscreened mobility due to interface roughness scattering is presented along with the mobility due to alloy scattering. When the second electronic subband becomes populated (Subsection 2.3.2.) we investigate the intrasubband and the intersubband scattering due to interface roughness.

Section 2.4. looks at a different kind of wire. It looks at DNA as a "molecular wire". A theoretical model appropriate for multiphonon-assisted small polaron transport through a disordered one-dimensional medium, is presented. A systematic derivation of an analytical expression for the electrical conductivity and the hopping distance as functions of the temperature, interpreting in a consistent way charge transport along the DNA "molecular wire", is given. In Subsection 2.4.1. the "microscopic" treatment is analyzed and in Subsection 2.4.2. percolation arguments lead to an analytical expression for the maximum hopping distance and the macroscopically observed electrical conductivity.

Chapter 3 deals with heterostructures of dimensions lower than one. It refers to Quantum Dots, often called artificial atoms, focused on their near-field magnetoabsorption spectra. The effect of an external magnetic field of variable orientation and magnitude on the linear near-field optical absorption spectra of single and coupled III-V semiconductor quantum dots is discussed. The study is focused on the spatial as well as on the magnetic confinement, varying the dimensions of the quantum dots and the magnetic field. The effect of the magnetic field on the absorption spectra, increasing the near-field illumination spot, is also investigated. The influence of the Coulomb interactions on the absorption spectra is also discussed. In Section 3.1. the theoretical framework is given. Subsection 3.1.1. is devoted to the calculation of the single particle states, Subsection 3.1.2. to the calculation of the Coulomb matrix elements), Subsection 3.1.3. to the formation of the excitonic problem and Subsection 3.1.4. to the calculation of the near field absorption spectra-spatial resolution. In Section 3.2. the theoretical analysis is applied to single and double QDs. Specifically, for the single particle states the effect of the spatial confinement vs. the magnetic field orientation and magnitude is discussed in the Subsection 3.2.1.. The influence of the Coulomb interaction on a single QD in *ideal* configuration is presented in Subsection 3.2.2., while results concerning singe QDs subjected to higher magnetic fields, double QDs with soft barrier and the ground state exciton binding is discussed in Subsections 3.2.3., 3.2.4. and 3.2.5., respectively.

Chapter 4 presents aspects of the magnetothermoelectric transport in the fractional Quantum Hall effect regime. The composite fermion picture, is briefly given in Section 4.1.. In Section 4.2. the theoretical framework for the calculation of the resistivity, the thermopower and the thermal conductivity for two dimensional electron and hole gases, at low temperatures and strong magnetic fields is outlined. Specifically, the idea of the parallel conduction, described in Subsection 4.2.1., enables us to use integer Quantum Hall effect models and Shubnikov-de Haas conductivity models (presented in Subsection 4.2.2.) for a quantitative comparison with experiment. General expressions for the transport coefficients are given in Subsection 4.2.3.. Electrical and thermal transport of composite fermions is

discussed in Section 4.3.. The calculations of the resistivity and the thermopower around filling factor $\nu = 1/2$ are presented in Subsection 4.3.1. and Subsection 4.3.3., respectively. The calculation of the resistivity around $\nu = 3/2$ (Subsection 4.3.2.) is also given. Finally, in a systematic way the range of the validity of the Wiedemann-Franz law in the integer quantum Hall effect regime is investigated in Section 4.4. for the diagonal (Subsection 4.4.1.) and the non-diagonal components (Subsection 4.4.2.)) of the thermal conductivity.

Throughout the book the theoretical results are compared with the existing experimental data accompanied with detailed discussions. Extensive bibliography and comments are also given for the experimental and theoretical research developments related with the specific topics.

The theoretical models proposed in this book and the results presented are mainly the product of the research work in recent years of the "Theory Group for the Study of Low Dimensional Semiconductor Heterostructures" of the Solid State Section of the Physics Department in the University of Athens (Greece). The author wishes to express his appreciation to his colleagues, Dr C. D. Simserides, Dr. V. C. Karavolas, Dr G. Hionis, Dr. M. Tsetseri, Dr M. Tsaousidou, Dr X. Zianni, Mrs (Msc) A. Zora for their fruitful and joyful collaboration during their participation in the research activities of the group, and their deep devotion to Physics.

Many thanks to my wife Giota and my daughter Maria for their understanding all these years.

Contents

Chapter 1

Quantum Wells

1.1. $Al_xGa_{1-x}As/GaAs/Al_xGa_{1-x}As$ Quantum Wells

1.1.1. Electron States

The quasi two-dimensional electron gas (Q2DEG) which accumulates at the GaAs side of a $n - Al_xGa_{l-x}As/GaAs$ selectively-doped single heterojunction (SD-SH) exhibits high electron mobilities, especially at low temperatures [14]- [16]. However, for the sheet electron concentration, N_s, which also plays a fundamental role in determining the channel conductivity, a maximum obtainable value has been found to exist (not larger than $1 \times 10^{12} cm^{-2}$), which depends on the structural parameters of the heterojunction [17]. An alternative and more effective approach to achieve higher N_s than such a limit, is to use a selectively-doped double heterojunction (SD-DH) [18]- [24]. Several theoretical methods have been presented in the literature (variational etc), but the most reliable among them are the self-consistent calculations for heterojunctions [25]- [29] and SD-DH [18]- [22], [30].

A model that depends only on the material parameters, was firstly introduced for the case of selectively doped single heterojunctions in [29]. This model was generalized for selectively doped double heterojunctions, bridging the heterojunctions with the SD-DH structures [31][1]. We will analyze it in the following. A similar model was used in the study of the effect of delta doping in double heterojunctions [32]. These models were presented at T = 0 K and they used the depletion approximation. Similar models have been successfully used to study the electronic structure of $A1_xGa_{1-x}As/GaAs/A1_xGa_{1-x}As$ quantum wells subjected to magnetic fields [33]- [35]. Important changes induced to the *famous* step-like form density of states of a Q2DEG when it is subjected to an in-plane magnetic field have also been reported [36].

A. Description of the System

In Fig. (1.1)(lhs) a schematic energy diagram of the valence and the conduction band of a $n - Al_xGa_{1-x}As/GaAs/n - Al_xGa_{1-x}As$ system (the SD-DH structure) is presented for the case in which the materials are considered to be separated. The GaAs well width is

[1] Reprinted from Simserides, C. D.; Triberis, G. P. J Phys Condens Matter, **5**, 6437, Copyright (1993), with permission from IOP.

$2L$. The $Al_xGa_{1-x}As$ layers, which have finite length, are uniformly doped with donors of concentration N_d, except from the two spacer layers of width D_s from both sides of the GaAs well. The donor levels are all supposed to lie at an energy ΔE_d below the bottom of the $Al_xGa_{1-x}As$ conduction band. All layers have a small unintentional acceptor doping N_a. The acceptor levels are supposed to lie at an energy ΔE_a above the top of the valence band, although the exact value of ΔE_a is of no interest here. $\Delta E_c = U_0$, and ΔE_v, are the conduction and the valence band offsets, respectively. The layers, considered separated above, are joined to form the heterostructure.

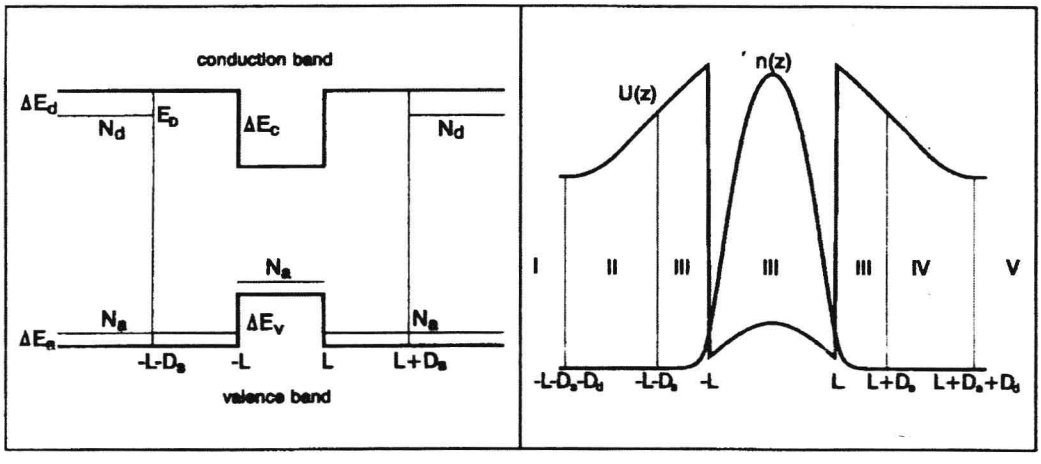

Figure 1.1. Schematic energy diagram of a SD-DH structure. [31]

Electrons are moving from the higher lying donor energy levels to the lower lying conduction band and acceptor levels of GaAs. This redistribution of carriers results in the formation of (i) region III which consists of the spacers and the GaAs layer with negative space charge due to ionized acceptors, (ii) regions II and IV, each of width D_d with positive space charge due to ionized donors ($N_a < N_d$) and (iii) regions I, V where there is no space charge. The electrons are mainly distributed in the well and their concentration, $n(z)$, which depends only on the coordinate z perpendicular to the interfaces, decays into the barriers, being zero at regions I and V. The qualitative diagram of the conduction band is given in Fig. (1.1)(rhs).

This redistribution of charges causes, together with the potential energy discontinuities and the exchange correlation potential energy, U_{xc} what is known as "band bending". This is also shown in Fig. (1.1)(rhs).

The charge density is given by

$$\rho(z) = \begin{cases} -en(z) & region\ I: & z \leq -[D_d + D_s + L] \\ e[N_d - N_a - n(z)] & region\ II: & -[D_d + D_s + L] < z \leq -[D_s + L] \\ -e[N_a + n(z)] & region\ III: & -[D_s + L] < z \leq [D_s + L] \\ e[N_d - N_a - n(z)] & region\ IV: & [D_s + L] < z \leq [D_d + D_s + L] \\ -en(z) & region\ V: & z > [D_d + D_s + L] \end{cases} \tag{1.1}$$

For realistic values of N_d, all the GaAs layer and spacers are completely depleted. $n(z)$

in regions I, V, as we have already stated, is zero.

The total potential energy is

$$U(z) = U_c + U_{band\ offset} + U_{xc} \tag{1.2}$$

where $U_c(z)$ is the Coulomb potential energy, obtained from the solution of the Poisson equation

$$\frac{d^2U_c}{dz^2} = \frac{e\rho(z)}{\epsilon_0\epsilon} \tag{1.3}$$

where, $-e$ is the electron charge, ϵ_0 and ϵ, are the vacuum and the relative dielectric constants, respectively. $U_{band\ offset}$ is U_0 for the $Al_xGa_{1-x}As$ layers and zero for the GaAs layer i.e. it is the potential energy discontinuity term. The formation of interfaces retains constant the band offsets as long as (i) interfaces are abrupt (ii) band offsets and electron affinities are independent of N_d and N_a, and (iii) no surface charges or dipoles are formed [37]. For U_{xc} we adopt the expression [29]

$$U_{xc} = -0.0783(\frac{e^2}{\epsilon_0\epsilon})[n(z)]^{\frac{1}{3}} \tag{1.4}$$

which is the dominant term (over 90%) in the full expression given in [27]. U_{xc} is not neglected because it has a small but not negligible influence on the sheet electron concentration [25]. According to calculations [31], this is $4-5\%$. We ignore the image potential energy term [27], because the difference in the dielectric constants of $Al_{0.3}Ga_{0.7}As$ and GaAs is very small. The exact potential energy depends on the specific electron gas distribution. The electron distribution reshapes the well, while it, itself, is reshaped by the shape of the well.

B. Self-consistent Calculations

The above discussion imposes the necessity of simultaneous solution of Schrödinger and Poisson equations. Starting from the Schrödinger equation, applying the effective mass approximation [38], taking into account the fact that the $Al_xGa_{1-x}As$ effective mass is different from the GaAs effective mass one should use the BenDaniel-Duke equation [39]. However, the penetration of the envelope function into the $Al_xGa_{1-x}As$ layers turns out to be small, and consequently we can use the value of GaAs effective mass, m^* (= $0.067m_e$, m_e being the free electron mass) throughout our system. This assumption results in a Schrödinger-like equation, where variables can be separated.

The electron density at T = 0 K (postulating $E_F = 0$) is

$$n(z) = -\sum_{i,occupied} \frac{m^*E_i}{\pi\hbar^2}|\zeta_i(z)|^2 \tag{1.5}$$

where $\zeta_i(z)$ is the z-axis envelope function with corresponding eigenvalues E_i. $\hbar$ is the reduced Planck constant.

It is now necessary to determine the asymptotic behavior of the potential energy $U(z)$ in the bulk material, away from the well i.e. in the regions I and V, and impose the boundary conditions for the envelope functions. At T = 0 K, E_F can be chosen as the highest

populated level. Clearly, this is the donor level E_D thus, $E_F = E_D$. Then, the energy distance between the Fermi level and the bottom of the conduction band is ΔE_d. We have already postdated $E_F = 0$. Therefore the asymptotic values of the potential energy are $U(bulk) = \Delta E_d$. On the other hand, $\zeta_i(z)$ decay exponentially in regions I and V.

The algorithm used to solve simultaneously the envelope function equation and the Poisson equation consists of the following steps (Fig. (1.2)):

(i) Start with an initial guess of the potential energy U_{in} (for example the band offsets' potential energy) and solve the one-dimensional Schrodinger-like z-axis envelope function equation. In this way, we obtain E_i and $\zeta_i(z)$.

(ii) Calculate $n(z)$ from Eq. (1.5).

(iii) The charge conservation equation gives

$$D_d = \frac{[N_s + 2(L + D_s)N_a]}{2(N_d - N_a)} \tag{1.6}$$

where the sheet electron density is

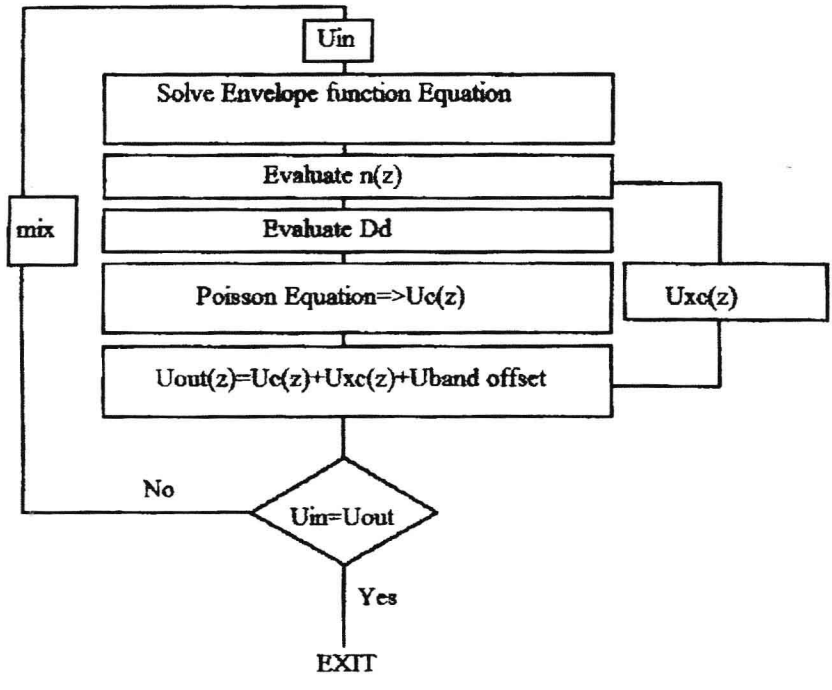

Figure 1.2. The algorithm chart for a self-consistent solution [31].

$$N_s = \int_{bulk(I)}^{bulk(V)} n(z)dz \tag{1.7}$$

(iv) Calculate $\rho(z)$ from Eq. (1.1).
(v) Obtain $U_c(z)$ solving Eq. (1.3).

In other words integrate $\rho(z)$ twice, starting from distant parts of the left and right sides of the $A1_xGa_{1-x}As$ layers (the bulk material), where there is no charge. D_d is usually much smaller than 100 $\mathring{A}$. In the present calculations its largest value does not exceed 600 $\mathring{A}$, thus, the boundary conditions for the Coulomb potential energy and its derivative are imposed at finite distance from each spacer. At bulk $U_{xc}(bulk) = 0, U_{(bulk)} = \Delta E_d$. Thus,

$$U_c(bulk) = \Delta E_d - U_0 \tag{1.8}$$

Also, in bulk $A1_xGa_{1-x}As$

$$(\frac{dU_c}{dz})(bulk) = 0 \tag{1.9}$$

(vi) Calculate $U_{xc}(z)$.
(vii) Calculate $U_{out} = U(z)$ from Eq.(1.2)
(viii) Is U_{out} "very close to" U_{in}? If not
(ix) Use Tchebycheff iteration scheme [40] to calculate new U_{in}, and so on, until the desired accuracy is succeeded.

The algorithm presented above is quite general for any SD-DH structure. Applying it to a specific $n - Al_xGa_{1-x}As/GaAs/n - Al_xGa_{1-x}As$ structure it is necessary to make some remarks concerning the values of the basic parameters involved in our calculations.

For Al mole fraction $x = 0.3$, the value we use, $\Delta E_c = 300meV$ is widely adopted [19, 29]. Furthermore, ΔE_d = 96 meV which is the experimental value for the Al mole fraction [41,42]. Here it should be noticed that this is a "mean" value averaging the shallow and D_x donors activation energies for this Al mole fraction [41]- [44]. The correct value of ΔE_d has not always been used in theoretical calculations, although it is of great importance. The use of smaller values for ΔE_d instead of the appropriate, for the specific Al mole fraction, lead to an overestimation of the sheet electron concentration [29, 45]. Studying the transition from "the perfect square well' to the double heterojunction" for both $Al_{0.3}Ga_{0.7}As$ and GaAs, for simplicity, we use the value of $Al_{0.3}Ga_{0.7}As$ dielectric constant i.e. 12.244. This results in a slight overestimation of N_s $(0.5 - 1\%)$. In the rest of the calculations we use the exact values of the $Al_{0.3}Ga_{0.7}As$ and GaAs dielectric constants i.e. 12.244 and 13.18, respectively. These values are obtained by interpolating AlAs and Gas dielectric constants [46]. In the following calculations, for simplicity we use $m^* = 0.067m_e$ i.e. its value for GaAs. This value is smaller than the one that should be used taking into account the small penetration of the envelope functions into the $Al_{0.3}Ga_{0.7}As$ layer. The sheet electron concentration remains constant as a function of temperature up to 100 K [15, 47]. This allows the comparison of the theoretical results with experiments performed at 4.2 K and 77 K.